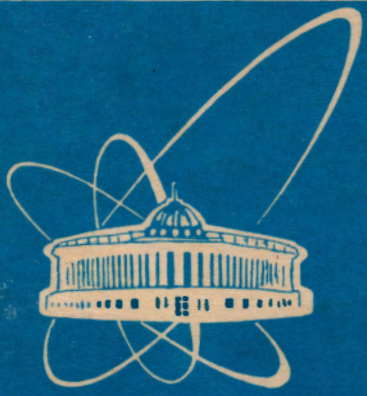

ОБЪЕДИНЕННЫЙ
ИНСТИТУТ
ЯДЕРНЫХ
ИССЛЕДОВАНИЙ

Дубна

E1-96-50

«THERMAL» MULTIFRAGMENTATION INDUCED IN GOLD TARGET BY RELATIVISTIC PROTONS

Submitted to «Physics Letters»

1996

V.A.Karnaukhov, S.P.Avdeyev, W.D.Kuznetsov, L.A.Petrov,
V.K.Rodionov, S.Y.Shmakov, V.V.Uzhinski, A.S.Zubkevich
Joint Institute for Nuclear Research, Dubna

H.Oeschler
IFK, Technishe Hochschule Darmstadt, 64289, Darmstadt, Germany

O.V.Bochkarev, L.V.Chulkov, E.A.Kuzmin, G.B.Yankov
Kurchatov Institute, 123182, Moscow, Russia

A.Budzanowski, W.Karcz
H.Niewodniczanski Institute of Nuclear Physics, 31—342, Cracow, Poland

E.Norbeck
University of Iowa, Iowa City, IA 52242 USA

The investigation of decay of very hot nuclei has become a topic of great interest. It is largely concentrated on the process of multiple emission of intermediate mass fragments (IMF, $3 \leq Z \leq 20$). Now it is established as the main decay mode of highly excited nuclei, and this process is likely to occur when a nucleus has expanded and lower density is reached [1]. It is under debate whether this process is related to a liquid-gas phase transition in nuclear matter [2–4].

The common way to produce very hot nuclei is to use reactions induced by heavy ions at energies $30 \div 100$ MeV/nucleon. But heating in this case is accompanied by compression, strong rotation and shape distortion, which cause the so-called dynamic effects in the nuclear decay. It seems difficult to disentangle all these effects to get information on thermodynamic properties of a hot nuclear system. The picture becomes clearer when light relativistic projectiles are used [5–7]. One should expect that dynamic effects are negligible in that case. All the IMF's are emitted by the only source — a target spectator, and decay of this hot nucleus proceeds in an apparently statistical manner ("thermal multifragmentation"). Similar advantages are given by antiproton beams of energy (1-2) GeV [8]. Light projectiles provide information complementary to that gained from heavy ion collisions, and the comparison will reveal the influence of compression and rotation on the multifragment decay of a hot nucleus.

In this paper we present the experimental results for the multifragment emission induced by relativistic protons in a gold target. The experiments were performed at the JINR synchrophasotron in Dubna using the modified 4π-set-up FASA [9]. The main parts of device are: (i) a fragment multiplicity detector (FMD) consisting of 64 thin (20 mg/cm^2) CsI(Tl) counters which cover a major part of 4π; the FMD gives the number of IMF's in the event and their space distribution; (ii) five Δ E (gas) $\times$ E (Si)-telescopes, which serve as a trigger for the readout of the system allowing measurement of the charge and energy distributions of IMF's at different angles. The calculated efficiency of the FMD for IMF detection is around 46%, while

the admixture of lighter particles to the counting rate is ≈ 3% with respect to IMF's. A self-supporting Au target 1.5 mg/cm^2 thick was used. The average beam intensity was $7 \cdot 10^8$ p/spill (spill length 300 ms, spill period 10 s).

Experiments have been performed at beam energies of 2.16, 3.6, 8.1 GeV. The measured multiplicity distributions associated with trigger fragments are shown in Fig. 1a. To deduce the primary multiplicity one should make corrections to the FMD efficiency, for the effect of double hits in the scintillators. Furthermore, one has to take into account the fact that the readout is triggered by telescopes with a small solid angle, so the trigger probability is proportional to the IMF multiplicity. All these effects are combined in a response matrix. The mean primary multiplicity is determined by fitting the parametrized distribution, folded by the experimental filter, to the experimental one. A reasonable assumption should be made for the shape of the primary distribution. In the case of definite excitation energy the multiplicity distributions are well described by the Poisson function with the mean value decreasing as the impact parameter increases [10]. In the present experiments we deal with fragmentation events averaged over the full range of impact parameters. Having this in mind we assumed the primary IMF-multiplicity distribution to be shaped like a Fermi distribution. Figure 1b presents the primary multiplicity distributions, which correspond to the best fit to the measured ones. The mean values $< M_{IMF} >$ (for events with at least one IMF) are 2.05±0.30, 2.6±0.4, 3.06±0.45 for the beam energies used. Corrections for double hits do not change $< M >$ by more than several percent but improve the fit at the tail of the multiplicity distribution. The errors (15%) are significantly larger than statistical ones reflecting the uncertainties in the FMD-efficiency.

Figure 2 shows the mean IMF–multiplicities as a function of projectile energy together with some published data on multifragmentation induced in Au-target by heavy ions ^{40}Ar (30 MeV/nucleon) [11], ^{36}Ar (110 MeV/nucleon) [12], ^{129}Xe (50 MeV/ nucleon) [10], ^{12}C (600 MeV/nucleon) [13]. The data were reanalyzed to get

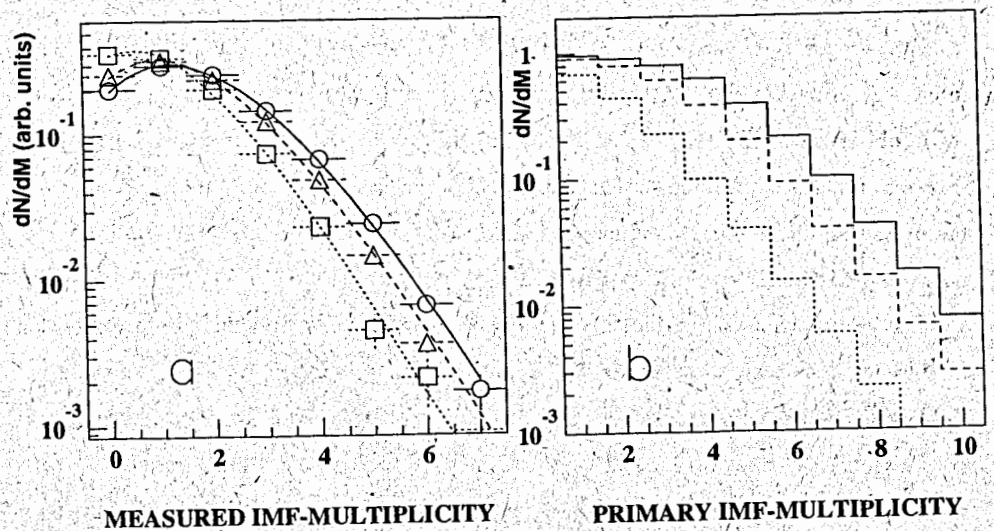

Fig. 1. Left: Measured IMF-multiplicity distributions associated with a trigger fragment of charge $6 \leq Z \leq 20$ for p+Au collisions at 8.1 GeV (circles, solid line), 3.6 GeV (triangles, dashed line), 2.16 GeV (squares, dotted line). They are fitted with Fermi-like distributions (right picture), folded with the experimental filter.

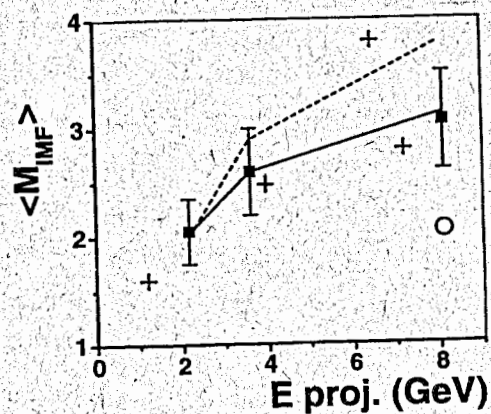

Fig. 2. The mean IMF multiplicities as a function of the beam energy. Solid points are for p+Au collisions, crosses are for fragmentation induced by ^{40}Ar, ^{36}Ar, ^{129}Xe and ^{12}C. The lines are drawn through the values calculated with MG+SMM (solid) and INC+SMM (dashed) at the proton energies used. The open point is calculated assuming preequilibrium emission after an intranuclear cascade.

$< M_{IMF} >$ for the events with at least one IMF averaged over the whole range of impact parameters. The IMF multiplicities for proton-induced reactions are close to those obtained with (^{12}C – ^{40}Ar) ions. So, this observable is not sensitive to the reaction dynamics and, one should think, it is determined mainly by the space phase factor of the final state. The enhanced $< M_{IMF} >$ value for ^{129}Xe + Au collision is caused by the larger size of the system.

The reaction mechanism for the relativistic projectiles is divided into two steps. The first one consists of a fast energy deposition stage, during which very energetic light particles are emitted and the nuclear remnant (spectator) is excited. The second one is the decay of a target spectator. The fast stage is usually described by the intranuclear cascade model (INC). We use a version of the INC from ref. [14] to get the distributions of the nuclear remnants in charge, mass and excitation energy. The second stage is described by the statistical multifragmentation model (SMM) [15]. The statistical behaviour of a target spectator is evident from the fact that the angular distributions of IMF's and their energy spectra at different angles are well described in the framework of the statistical decay of a thermalized moving source [16]. Within the SMM the probabilities of different decay channels are proportional to their statistical weights. The break-up volume determining the Coulomb energy of the system is taken to be $V_b = (1 + k)A/\rho_o$, where A is the mass number of the decaying nucleus, ρ_o is the normal nuclear density, k is a model parameter. So, thermal expansion of the system before the break-up is assumed. The primary fragments are hot, and their deexcitation is taken into account to get final IMF distributions. In further calculations we use $k = 2$ based on our analysis of the correlation data [17]. This value corresponds to the break-up density $\rho_b \approx 1/3\rho_o$. The upper dashed line in Fig. 2 is obtained by means of this combined model. The calculated mean multiplicity for the highest energy is 25% larger than the experimental one indicating an overestimation of the excitation energy of the residual nucleus. For the lowest beam energy the calculated $< M_{IMF} >$ coincides with the measured one. The use of the preequilibrium

exciton model (PE) [18] together with the INC gives a mean multiplicity 33% less than the experimental value for $E_p = 8.1$ GeV. So, the use of the INC or INC+PE does not solve the problem of describing the properties of a target spectator for a wide range of projectile energies, and one should look for an alternative approach. The authors of [19] came to the same conclusion and used some phenomenological distributions to describe the experimental data. Unfortunately, there is no simple way to extend their results to other projectile/target combinations.

To find charge, mass and energy distributions of the residual nuclei we used the well-known Glauber theory [20] as a basis, which is in good agreement with the experimental data on elastic and inelastic hadron-nucleus (hA) and nucleus-nucleus (AA) interactions at intermediate and high energies. However, the Glauber theory, as it is, provides only the distribution of knocked-out nucleons resulting from the primary collisions of the projectile nucleons with the target ones and does not take into account the secondary interactions of ejected nucleons. To take such interactions into consideration a phenomenological approach was used [21], motivated by the Regge theory of hA and AA interactions. Considering the so-called "enhanced diagrams" [22] this approach provides an alternative to the cascade model. The full implementation of the Regge picture is rather complicated, but it can be reproduced by ejecting additional nucleons placed not far from the primary ejected ones in the impact parameter plane. So, the knock-out of the nucleons with impact parameter $\vec{s}$ initiates the knock-out of neighboring nucleons with impact parameters $\vec{s}_j$ with a probability $\phi(|\vec{s} - \vec{s}_j|)$. The second nucleon, in its turn, can initiate a knock-out of a third nucleon with a probability $\phi(|\vec{s}_j - \vec{s}_k|)$ and so on. The probability function $\phi(|\vec{s}_j - \vec{s}_k|)$ is chosen in the Gaussian form to reproduce behaviour of the simplest enhanced hA–interaction diagram. The parameters of the function are determined from the data on g-particle multiplicities in inelastic interaction of 3.6 GeV/nucleon protons and nuclei with light and heavy components of emulsion. The space coordinates of the primary ejected nucleons are determined by the code implementing exact

Glauber relations for pA and AA interactions [23]. To calculate the excitation energy of the nuclear residual we suppose that each spectator nucleon placed at a distance less than 2 fm from a nucleon touched at the fast stage of the interaction receives an energy distributed as $P(\varepsilon)d\varepsilon = <\varepsilon>^{-1} exp(-\varepsilon/<\varepsilon>)d\varepsilon$. A sum of the energies transferred to the spectator nucleons gives the excitation energy. Below we will refer to that approach as a modified Glauber approach (MG). Within this model followed by SMM the mean IMF-multiplicities are calculated by varying the values of $<\varepsilon>$. The best fit to the experimental data is obtained for $<\varepsilon>$ equal to 6, 8 and 10 MeV at the beam energies 2.16, 3.6 and 8.1 GeV, respectively.

Table 1 summarizes the results of the calculations with INC+SMM and MG+SMM. The mean charge (Z_{MF}) and mass (A_{MF}) of the target spectator decaying with emission of at least one IMF are lower than mean Z_R and A_R of residual nuclei averaged over all inelastic events (INC: $Z_R = 74$, $A_R = 180$ for $E_p = 8.1$ GeV and $Z_R = 77$, $A_R = 188$ for $E_p = 2.16$ GeV; MG: $Z_R = 75$, $A_R = 186$ for all the beam energies used). This means that only hard collisions contribute to the multifragmentation process. At the same time the mean excitation energy of the fragmenting remnant E^*_{MF} is larger than the mean excitation energy E^*_R for all residual nuclei. The mean charge and mass numbers of the fragmenting nuclei grow with the decrease of the beam energy in the INC+SMM model. The opposite occurs for MG+SMM calculations. For the projectile energy 2.16 GeV both models give the same values for $<M_{IMF}>$, but Z and A of fragmenting nuclei differ significantly. These very different predictions can be judged by comparison of the measured and calculated IMF-energy spectra, as they are mainly determined by the charge and size of the source.

We obtain the energy spectra by calculating the classical multibody Coulomb trajectories using a code developed in [24] (for all the charged particles in the event given by SMM). The initial coordinates of the particle centers are randomly generated inside the break-up volume, the initial momenta are randomly generated according to the maxwellian distribution at the temperature given by the model. The trajectories

Table 1: The calculated properties of the nuclear remnants in p+Au collisions

Reaction	Experiment	Calculations					Model
	$<M_{IMF}>$	$<M_{IMF}>$	Z_{MF}	A_{MF}	$E^*_{MF}MeV$	E^*_RMeV	
p+Au		3.8	70	168	911	524	INC+SMM
8.1 GeV	3.06±0.45	2.05	50	122	528	204	INC+PE+SMM
		3.13	67	165	780	279	MG+SMM
p+Au	2.6+0.4	2.9	73	176	757	407	INC+SMM
3.6 GeV		2.6	65	162	677	225	MG+SMM
p+Au	2.05±0.30	2.0	75	181	642	328	INC+SMM
2.16 GeV		2.03	64	157	574	164	MG+SMM

Z_{MF}, A_{MF}, E^*_{MF} are the mean charge, mass number and excitation energy of the fragmenting nucleus. E^*_R is the mean excitation energy of all residual nuclei after the fast stage of a collision.

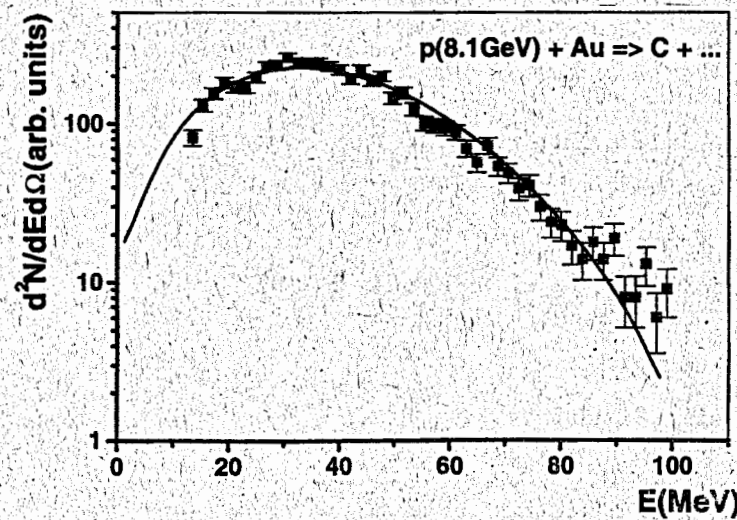

Fig. 3. The energy spectrum for carbon emitted in p(8.1 GeV) + Au collisions. The line is calculated with the modified Glauber approach and statistical multifragmentation model.

are followed step by step up to $t = 3000$ fm/c, when the fragment energy reaches $\approx$ 98% of the asymptotic value. Fig. 3 illustrates the quality of the model description of the carbon energy spectrum measured at $\Theta = 87°$. The statistical model assumes that the break-up of the system proceeds after an expansion driven by a thermal pressure, but the expansion velocity v_{exp} is neglected. So, the comparison of the measured IMF energies with the calculated ones is the way to estimate v_{exp}. In our case the effect of the expansion velocity is not visible and only the upper limit of it can be extracted: $v_{exp} \leq 0.03$ c. -Fig. 4 presents the comparison of the measured mean IMF-energies (corrected for the detection threshold E/A = 1.2 MeV) with the calculated ones. Let us first consider the region of $Z_{IMF} \leq 9$. Here the experimental data follow the predictions of MG+SMM. The calculations with INC+SMM at $E_p = 2.16$ GeV give the mean IMF-energies definitely higher than the experimental ones reflecting a model overestimation of the source charge. So, the modified Glauber approach gives a more adequate description of the properties of nuclear remnants after the fast stage of the reaction. The measured mean energies for $Z_{IMF} > 9$ are lower than the calculated ones (more pronounced at $E_p = 8.1$ GeV). We believe this observation indicates the failure of the model assumption that the fragments have equal probabilities to be formed at any available place inside the break-up volume. In fact, the interior of the expanded nucleus is favored over the diffuse edge for the appearance of larger IMF's as the fragments are formed via the density fluctuations. This results in lower Coulomb energies for them with respect to the model prediction. This observation presents additional evidence for the volume emission of the fragments. A similar conclusion was made in [25].

Concluding, we have shown that in collisions of (2-8) GeV protons with gold very excited target spectators are created, which decay via multiple emission of intermediate mass fragments. The mean IMF–multiplicities are comparable with those obtained with heavy ions (^{12}C-^{40}Ar) in the same energy range. So, this observable is not sensitive to the reaction dynamics. The IMF–multiplicity and energy distributions are analyzed in the framework of a combined model, which includes the modified Glauber approach for the fast stage of the reaction and the statistical multifragmentation model neglecting the dynamics of the thermal expansion of the remnant. The model adequately describes the properties of a remnant system. The IMF–energy spectra are consistent with the calculations up to $Z_{IMF} = 9$ and the expansion velocity is estimated to be less than 0.03 c. The present results support a scenario of true thermal multifragmentation of a hot and expanded nuclear system.

The authors are thankful to Profs A. Hrynkiewicz, A.M. Baldin, S.T. Belyaev, A. Sissakian and E. Kankeleit for support. The research was supported in part by Grant No.RFK300 from the International Science Foundation and Russian Government, Grant No.93-02-3755 from the Russian Fundamental Research Foundation, by Grant No.94-2249 from INTAS, by Grant No.2P30B 09509 from the Polish State Committee for Scientific Research, by contract No.06DA453 with Bundesministerium für Forschung und Technologie and by the US National Science Foundation.

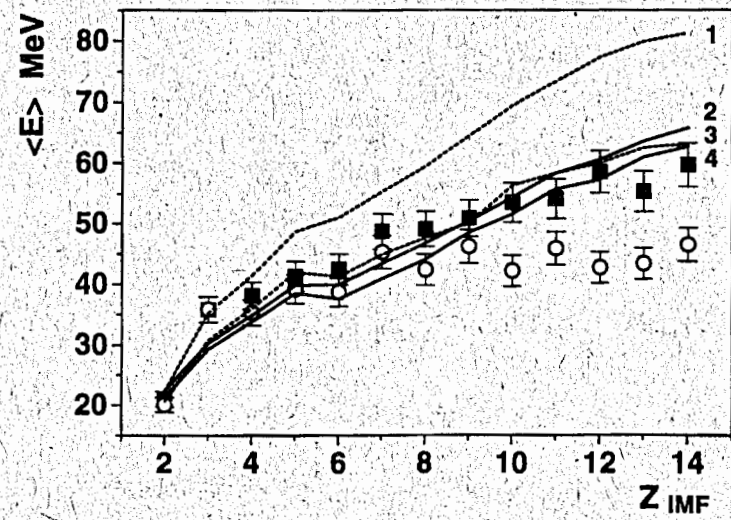

Fig. 4. The mean energies of fragments in p+Au collisions at 2.16 GeV (solid points, dashed lines) and 8.1 GeV (open points, solid lines). The lines are calculated with INC+SMM (1,2) and MG+SMM (3,4).

References

1. "Multifragmentation", Proceedings of the Int. Workshop XXII on Gross Properties of Nucl. Excit., Hirschegg, Austria, 1994, Ed. by H. Feldmeier and W. Nörenberg, GSI, Darmstadt, 1994.
2. J. Bondorf, et al. Nucl. Phys. A444 (1985) 460.
3. D.H.E. Gross, Nucl. Phys. A428 (1985) 313c.
4. J.Pochodzalla, et al. Phys. Rev. Lett. 75 (1995) 1040.
5. V. Lips, et al. Phys. Rev. Lett., 72 (1994) 1604.
6. L. Pienkowski, et al. Phys. Lett. B336 (1994) 147.
7. K. Kwiatkowski, et al. Phys. Rev. Lett. 74 (1995) 3756.
8. J. Cugnon, Yad. Fiz., 57 (1994) 1705.
9. S.P. Avdeyev, et al. Preprint JINR P13-95-256, Dubna, 1995; PTE in print.
10. D.R. Bowmann, et al. Phys. Rev. C46 (1992) 1834.
11. R. Trockel, et al. Phys. Rev. C39 (1989) 729.
12. R.T. de Souza, et al. Phys. Lett. B268 (1991) 6.
13. M. Begemann-Blaich, et al. Preprint GSI-93-29, Darmstadt, 1993.
14. V.D. Toneev, K.K. Gudima, Nucl. Phys. A400 (1983) 173c.
15. A.S. Botvina, A.S. Iljinov, I. Mishustin, Nucl. Phys. A507 (1990) 649.
16. V.A. Karnaukhov, et al. Preprint JINR E7-95-321, Dubna, 1995.
17. S.Y. Shmakov, et al. Yad. Fiz. 58, No 10 (1995) 1735.
18. M. Blann, Ann. Rev. Nucl. Sci., 25 (1975) 123.
19. A.S. Botvina, et al. Nucl. Phys., A584 (1995) 737.
20. R.J. Glauber, Proc. of the 2nd Int. Conf. on High Energy Physics and Nuclear Structure, (Rehovoth, 1967) Ed. G.A.Alexander, North-Holland, Amsterdam, 1967.
21. Kh. El-Waged, W.W. Uzhinskii, Preprint JINR E2-94-126, Dubna, 1994.
22. K.G. Boreskov, et al. Yad. Fiz., 53 (1991) 569.
23. S.Yu. Shmakov, et al. Comp. Phys. Commun., 54 (1989) 125.
24. P.G. Akishin, et al. Preprint JINR E11-94-140, Dubna, 1994.
25. A.S. Hirsch, et al. Phys. Rev. C29 (1984) 508.

Received by Publishing Department
on February 14, 1996.